ELSEVIER

Chemical Engineering Journal 89 (2002) 229–238

Chemical Engineering Journal

www.elsevier.com/locate/cej

Inclined wettable filter for mist purification

Igor E. Agranovski [a,*], Toshihiko Myojo [b], Roger D. Braddock [a], Darren Jarvis [a]

[a] *Faculty of Environmental Sciences, Griffith University, 4111 Brisbane, Qld, Australia*
[b] *National Institute of Industrial Health, Nagao, Tama, Kawasaki 214-8585, Japan*

Abstract

Agranovski and Braddock [AIChE J. 4 (1998) 2784] investigated a process of filtration of ultra small liquid particles on wettable fibrous filters. They found that liquid droplets captured by a wettable filter spread along the fibres and create a thin liquid film covering each fibre. These films of liquid establish a self-draining, tapered equilibrium flow down the filter. The thickness of the liquid film is an important parameter altering the physical characteristics and performance of the filter. The properties of the film depend on the density, viscosity and amount of liquid present, the physical parameters, wettability and dimensions of the filter and also on the orientation and angle of inclination of the filter. The thickness of the liquid film can be increased by increasing the angle of inclination of the filter and by selecting the orientation. It leads to the possibility of increasing the efficiency of wet filtration without any increase in the amount of irrigating liquid involved. It is especially important for industries where, due to some technological or economical reasons, the amount of fresh irrigating liquid available for the process, is limited. In the current paper, the results of theoretical and experimental analysis of inclined wettable filtration systems are presented and further steps towards industrial design are discussed.

Keywords: Air purification; Air filter; Aerosols; Wettability; Mist removal; Filter clogging

1. Introduction

The rapid development of industrial processes has given rise to a need for highly efficient air quality control equipment. A variety of techniques, from low efficiency settling chambers to moderately efficient cyclones, wet methods and highly efficient filters, is available to meet local particulate emission requirements. However, there is now an alternative to the employment of filters where there is need for efficient removal (better than 99%) of particles in the 0.01–1 μm size range from any substantial flow of air [1].

Filtration of solid particles from gas streams is usually associated with the build up of solid porous deposits on the surface of a filter. These deposits are continuously (shaking of the filter) or periodically (reversed air jet) removed from the filter to keep the resistance of the device within design limits. However, besides the negative effects associated with elevated resistance and ultimately blockage, the deposits become an additional filtering media and increase the filtering efficiency of the device [2].

Filtration of liquid aerosols is a significantly different process. Deposits of liquid, created as the result of the capture of droplets, are not penetrable by gas streams and could cause significant alternations to the purification and aerodynamic properties of the filter. Also, filtration of liquid particles, unless viscous and sticky liquids are involved, does not require any filter regeneration techniques due to a self-cleaning nature of the process [3].

Agranovski and Braddock [4] showed that liquid particles collected by wettable fibrous filters spread along the fibres and, after steady-state conditions have been established, create a thin film covering each fibre. This essentially increases the fibre diameter and the packing density of the filter. Usually the thickness of the film depends on the properties and amount of the liquid supplied, the dimensions and arrangement of the filter, and the characteristics of the filter fibre. These thin films form drainage paths down the filter and provide a self-cleaning mechanism. Note, that these films can be enhanced, or artificially created, by spraying irrigating liquid through nozzles onto the filter, to enhance the capture of aerosols, either liquid or solid.

On the other hand, nonwettable fibrous filters can be best described as liquid-repellent filters [5]. The wetting/nonwetting material property depends on both the liquid and the material in the fibres. The main aspect in the nonwettable filtration process is that the captured liquid particles remain as spheres attached to the filter and grow as the result of coalescence with new incoming droplets. Once the attached sphere becomes large, the gravitational force

* Corresponding author. Tel.: +61-73875-7923; fax: +61-73875-7459.
E-mail address: i.agranovski@mailbox.gu.edu.au (I.E. Agranovski).

1385-8947/02/$ – see front matter © 2002 Elsevier Science B.V. All rights reserved.
PII: S1385-8947(02)00130-4

exceeds the force of adhesion and the drop simply falls from the filter.

Obviously, for most applications, water will be used as the liquid for artificial film generation. It can be supplied through a set of nozzles strategically arranged to ensure a required distribution along the filter. The filtered contaminants are then removed from the fibres by a continuous influx of fresh water, thus preventing blockages in the filter. To prevent blockages of the filter and nozzles, it is strongly recommended that fresh or at least filtered water be used as the make up fluid. Sometimes the irrigating fluid will be selected so as to have desirable chemical properties with respect to the aerosol being collected. For technological or economical reasons, the amount of fresh irrigating liquid available for filter irrigation is sometimes limited and below the design requirements. It can cause drying and possibly blocking of certain areas of the filter. To avoid this situation, some other mechanisms for keeping the film thickness within the design limits have to be identified.

Traditionally filters have been mounted in a vertical plane. The purpose of the paper is to study the effect of orientation of the filter at other angles, and the influence of inclination on the penetration of droplets, and the resistance of the filter. This paper uses experiments and theory to investigate the performance of inclined wettable filters and discusses some possibilities for utilisation of the technology for different applications.

2. Theoretical background

Liquid particles captured by wettable filters spread along fibres and generate thin films. The thickness and drainage velocity of the film covering a vertical wettable fibre can be estimated by the equations derived by Agranovski and Braddock [4]. These equations involve physical parameters such as viscosity, density and the rate of supply of liquid and were derived for vertically oriented filters. Now consider the experimental apparatus as shown in Fig. 1, where the filter box is oriented at angle θ to the horizontal. The airflow in the experiments was always directed from left to right (as shown in Fig. 1) and was normal to the filter. For clarity, we take θ as positive for a counterclockwise rotation of the filter box, and θ as negative for a clockwise rotation. The details of the experimental apparatus will be described shortly. For the inclined case, the effective component of gravity down the filter, is $g\cos\theta$, where g is the gravitational acceleration. The x-axis points down the filter surface and has its origin at the top of the filter. The other assumptions in the derivation by Agranovski and Braddock [4], including that the film's surface is parallel to the surface of the fibre, flow is steady-state and laminar, and flow parameters do not depend on the size of the fibre (curvature has not been taken into consideration), are still valid. Then the equation for the film thickness is:

$$\delta = \sqrt[0.33]{\frac{3G_f(x)\upsilon}{\rho^2 g\cos\theta}} \tag{1}$$

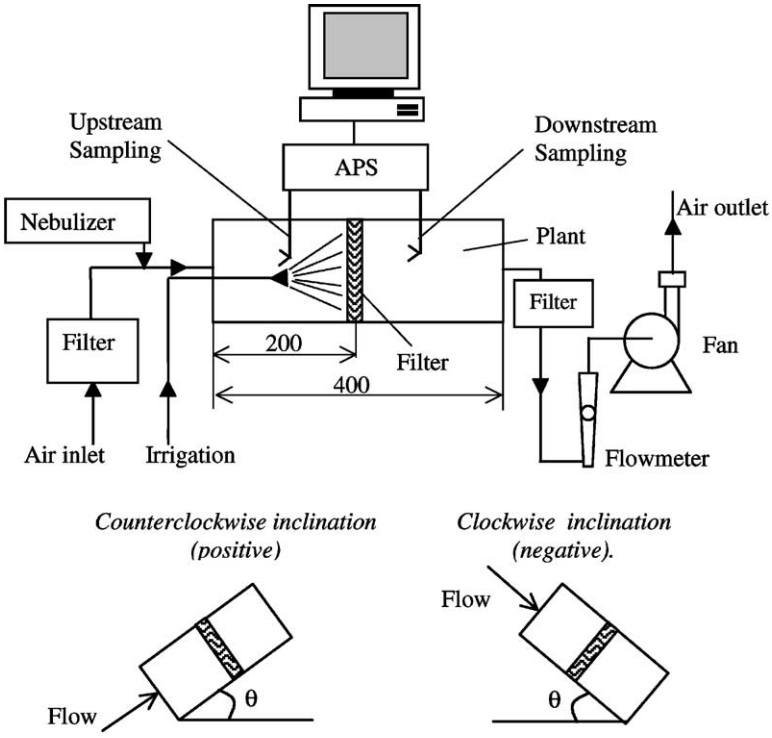

Fig. 1. Experimental plant.

where υ is the viscosity and ρ is the density of the liquid. G_f (x) is the mass of liquid captured by the liquid film on the length x of the fibre above the point, and G_f (x) is linearly related to the total amount of fluid G_L applied to the filter. Note, that because of the symmetry of the $\cos\theta$ function, Eq. (1) does not distinguish the direction of rotation or inclination. As discussed in Agranovski and Braddock [4], the theoretical results calculated by the Eq. (1) have been fully verified by the results of the experimental runs for the vertically arranged wettable filter. On this basis the simple theoretical approach described above has been accepted as an appropriate tool for the theoretical evaluation of the film thickness covering wettable fibre.

Agranovski and Braddock [4] found that the tapering effect in the fluid film is small. However, to avoid any potential problems related to taper, the experimental set-up was made as short as possible and equal to 180 mm. For this height, the difference between the thickness of the film at the top and bottom of the filter is negligibly small and the theoretical and measured efficiencies of the filter are almost the same [3].

The value of the packing density of the wetted filter is different from that for the dry regime; called "the dry packing density". Fibres covered by liquid are thicker than dry ones; obviously they occupy more space and increase the packing density of the filter. The term "equivalent packing density" will be used to describe the packing density of the wetted filter.

The equivalent packing density is calculated from the geometry of filter assuming the filter to be a system of parallel vertical cylinders in a regular hexagonal packing arrangement [6]. The thickness of the film for particular parameters of the process is calculated by Eq. (1) and the equivalent packing density is then calculated. There are few recently developed more sophisticated models describing filter structure [7,8] also available. However, the difference between results obtained from these models compared to the regular hexagonal model, does not exceed 10% [8].

The capture of particles can arise due to interception, inertia, diffusion, settling, thermophoresis and diffusiophoresis processes. The efficiency of the filter is estimated by using a single-fibre efficiency concept [1]. The theoretical efficiency of the single fibre for each process is readily estimated once the equivalent diameter of the fibres is known [2,4,6]. The removal processes are considered to be mutually exclusive and usually combined by arithmetic sum [6,9]. In estimating the overall single-fibre collection efficiency, it is necessary to include an interaction term, to account for enhanced collection due to interception of the diffusing particles [9]. Appropriate formulae for all removal mechanisms are given in Hinds [9]. Once the single-fibre efficiency is known, the theoretical total filter efficiency, E, can be estimated using

$$E = 1 - \exp\left(-\frac{2\eta c H}{\pi R}\right) \tag{2}$$

where η is a single-fibre efficiency, c the equivalent packing density, H the thickness of the filter, and R is the radius of the wetted fibre [9]. The theoretical penetration, P, is estimated as

$$P = 1 - E \tag{3}$$

3. Experiments

Experiments were conducted using the apparatus shown in Fig. 1. To visualise the process, a filter box with dimensions 400 mm × 300 mm × 100 mm was made out of transparent plastic. The box was also mounted on a plane, which could be inclined to the horizontal, in both clockwise and counterclockwise directions. The filter was fixed in the flange and located 200 mm from the entrance to the box. An ultrasonic nebulizer was utilised to generate distilled water particles in a range of sizes. Make up fluid could also be supplied through the nozzles, to ensure that the films were fully developed on the filter fibres. The irrigation rate was estimated as the total weight of droplets supplied by the nebulizer and nozzles, and transported by the air stream to the filter. The actual irrigation rate used in all of the experiments was 0.08 kg/h. A wettable filter made out of glass fibres with a diameter of 8 μm, dry packing density 3% and thickness 5 mm was involved in the investigation. The dimensions of the filter window were 180 mm vertically and 70 mm horizontally. A centrifugal fan, capable of supplying up to 450 l/min of air was used in the experiments. A float rotameter with adjusting valve was employed to monitor and control the airflow rate. A HEPA filter was located at the inlet point to remove all additives from the air to avoid their interference with the process. Standard upstream and downstream number concentration monitoring was performed using an Aerodynamic Particle Sizer (TSI). To avoid the influence of local air disturbances, geometrically identical sampling probes were located at least 100 mm from the air inlet to the plant (inlet sampling probe) and 100 mm from the back filter surface (outlet sampling probe). Same length (minimum possible) and diameter pipes were employed to connect probes with the monitoring instrument to eliminate any differences in results due to possible settlement of aerosol along the inner surfaces of the pipes. The experimental penetration was calculated as

$$\text{penetration} = \frac{\text{downstream number concentration}}{\text{upstream number concentration}} \times 100\% \tag{4}$$

The set-up also included instruments to monitor temperature and humidity of the air stream and pressure drop across the filter assembly. Pressure drop across the filter was measured as the difference between upstream and downstream static pressures by a 1 Pa resolution manometer. A nozzle, capable of generating water droplets with sizes around

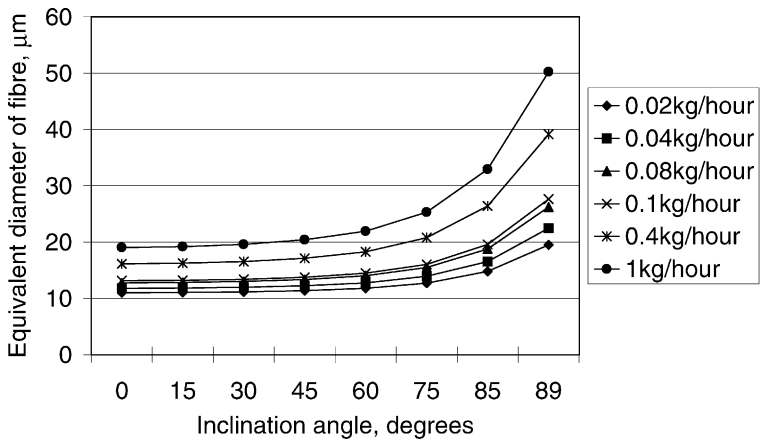

Fig. 2. Equivalent diameter of the wet fibre as function of inclination, for a range of total flow rates G_L.

60 μm provided an initial wetting or additional irrigation of the filter on request. The nozzle was located at the entrance to the box and directed parallel to and in the same direction as the air stream.

To investigate the performances of different arrangements, the experiments were conducted for angles: $\theta = 0^\circ$ (vertical), $\theta = +15$ and $+30^\circ$ (counterclockwise), and $\theta = -15$ and -30° (clockwise). Some 15 runs were made for each angle.

4. Results

4.1. Equivalent thickness of the film and packing density

The theoretical equivalent thickness of the film, and the theoretical packing density were calculated using Eq. (1), for a range of inclinations, $0 \leq \theta < 90^\circ$, and for theoretical irrigation rates of $0.02 \leq G_L \leq 1.0$ kg/h (see Figs. 2 and 3). Note the singularity at $\theta = \pm 90^\circ$, where the gravitational component along the fibre is zero.

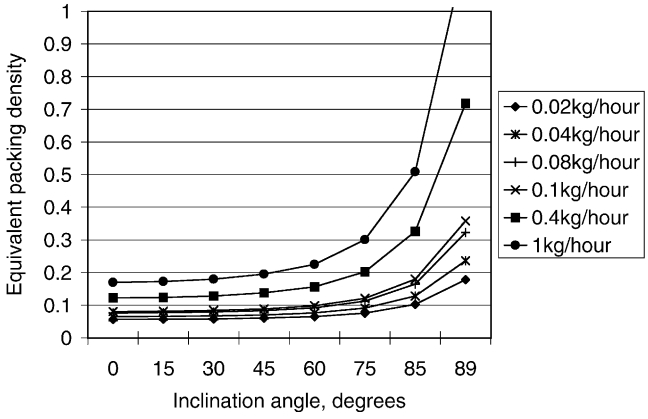

Fig. 3. Equivalent packing density of the wet fibre filter as function of inclination for a range of total flow rates.

As is seen from the graphs (see Fig. 2), the effective equilibrium diameter of the fibre is slowly increasing with θ from 0 to 60° and then increases more rapidly within the range from 60 to 89°. For some irrigation rates, the equivalent diameter at $\theta = 89^\circ$ is as much as 2.5 times the equivalent diameter at $\theta = 0^\circ$. For lower irrigation rates from 0.02 to 0.1 kg/h, the increase in the effective equivalent diameter from the vertical arrangement ($\theta = 0^\circ$) to the maximum inclination ($\theta = 89^\circ$) varies from 7 to 28%. For the highest irrigation rate of 1.0 kg/h, the increase in the equivalent diameter from $\theta = 0$ to 89°, is almost twice the increase in diameter obtained for the low flow rates; 0.02–0.1 kg/h.

The theoretical equivalent packing density has been calculated from the corresponding data on the equivalent diameters of the fibre and the results are shown in Fig. 3. For inclination angles of less than 60° and low irrigation rates, the packing density is increasing much more slowly than for inclinations above 60°. For most of the irrigation rates and angles, the equivalent packing density is less than 1, however for the highest irrigation rate of 1 kg/h the equivalent packing density is 1 for $\theta_C \approx 87.5^\circ$. Note that for large θ, the component of gravity normal to the fibres, is much larger than the gravity component along the fibres which significantly decreases the rate of drainage of liquid from the filter. For $\theta = \theta_C$, the situation arises where all neighbouring films coalesce and water occupies the whole space between the fibres of the filter (equivalent packing density is 1). Different physical processes need to be considered in these situations.

4.2. Pressure drop across the filter

The pressure drop across the filter as a function of time is shown in Fig. 4. The experiment started from a previously wet filter run, but with time starting from the switch to a different airflow value. The results shown in Fig. 4 were taken for the vertically arranged filter, the airflow rate of 100 l/min and the water flow rate of 0.08 kg/h, and show the average of 15 experimental runs. The error bars show the variability

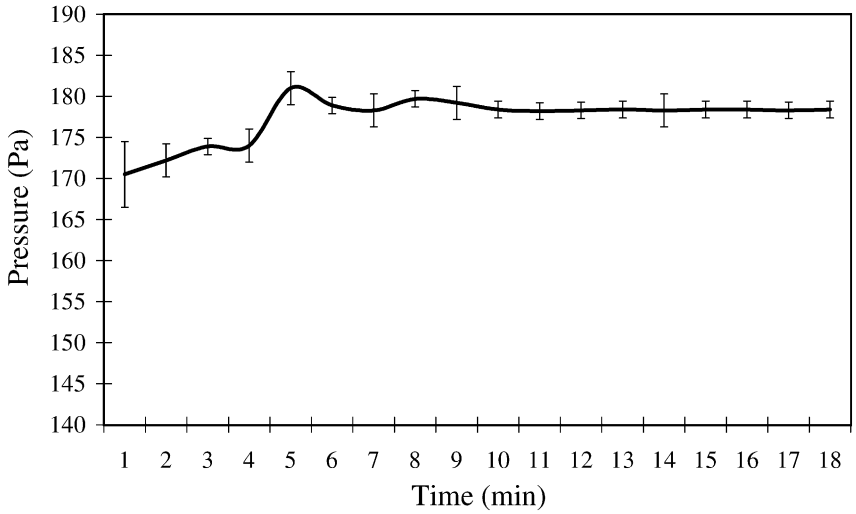

Fig. 4. Average pressure drop across the vertically arranged filter, as a function of time. Error bars represent STD of 15 experimental runs.

of the measurements. The results show some initial fluctuations in the pressure drop in the transition region, followed by stabilisation at the steady-state operating level. Generally the transition was accomplished in about 11 min on average. In the data collection experiments, at least 15 min had been allowed for stabilisation of the process before the actual measurement of the resistance was taken.

Both the theoretical and the average of the experimental (after 15 min stabilisation) results for the pressure drop across the filter are presented in Fig. 5. The theoretical results were calculated using the following equation [9]:

$$\Delta P = \frac{4\mu_g cUH}{R^2[c - 3/4 - (\ln c)/2 - c^2/4]} \quad (5)$$

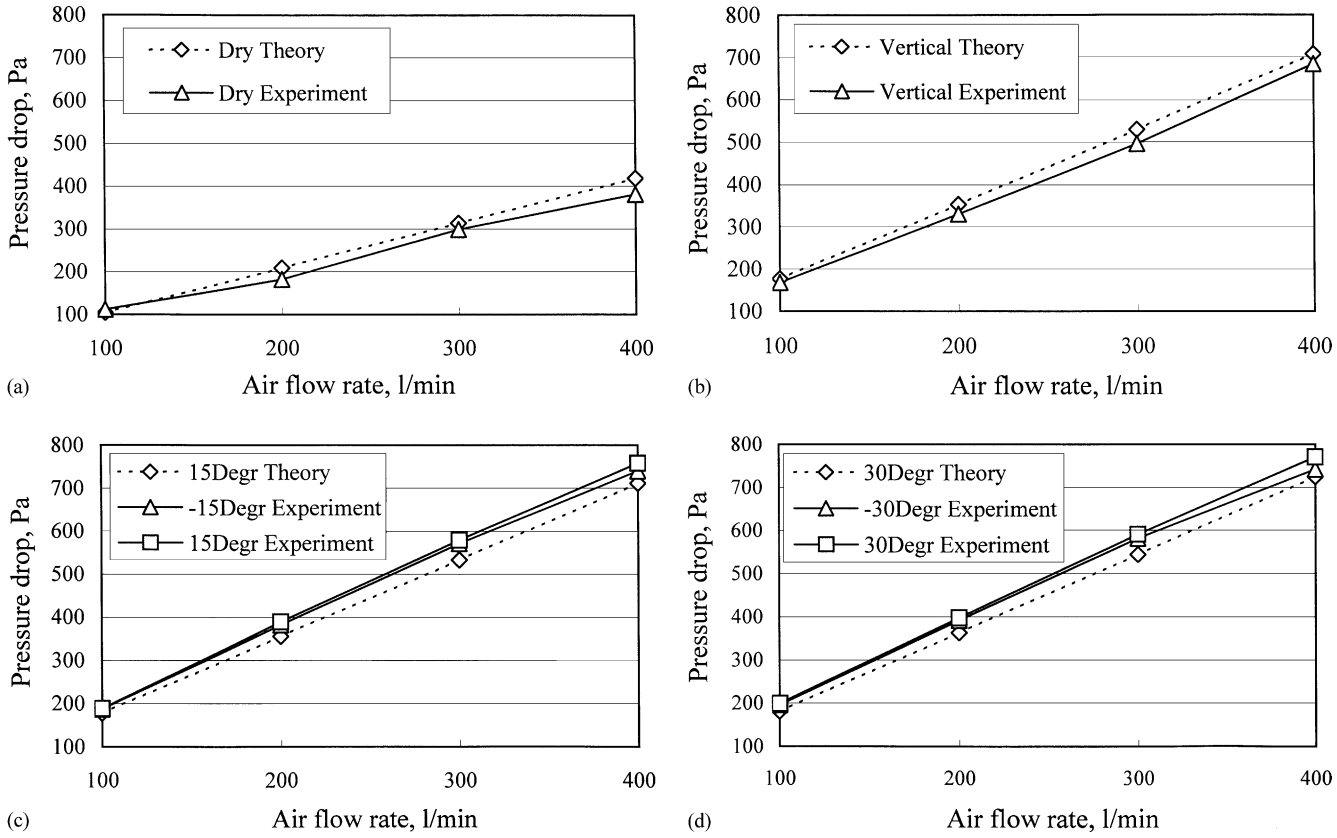

Fig. 5. Stabilised pressure drop across the filter as a function of the air flow rate, showing theoretical and measured values: (a) dry filter, (b) wet filter at $\theta = 0°$, (c) wet filter at $\theta = \pm 15°$, (d) wet filter at $\theta = \pm 30°$.

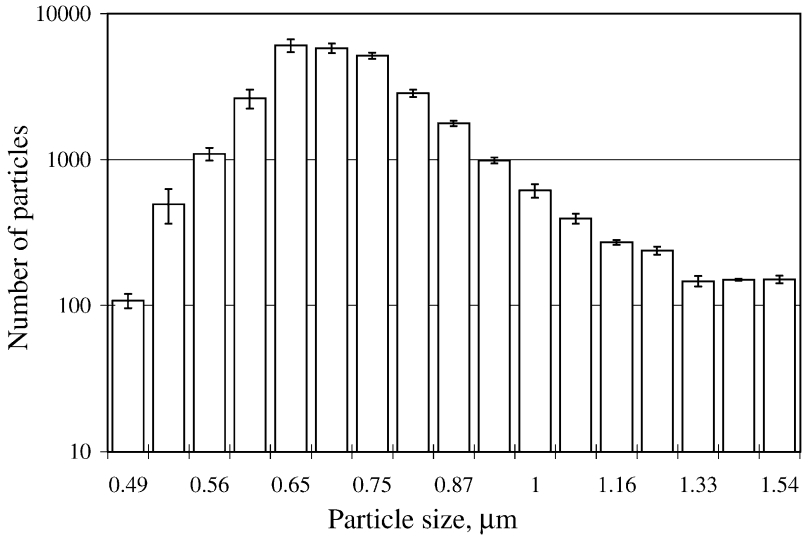

Fig. 6. Average size distribution of particles used in experiments. Error bars show experimental variation across 15 runs.

where μ_g is the gas viscosity and U is the gas face velocity. The theoretical model does not distinguish between positive and negative arrangements of the filter, and the theoretical results are presented for wet filters at $\theta = 0$, $+15$ and $+30^\circ$. The experimental results are presented for a dry filter, and for a wet filter arranged at $\theta = 0$, ± 15 and $\pm 30^\circ$. Airflow rates of 100, 200, 300 and 400 l/min correspond to face velocities of 16, 32, 48 and 64 cm/s. All experimental graphs show a linear relation between airflow rate and the stabilised pressure drop across the filter. The resistance of the wet filter is on average 1.7 times higher than the resistance of the dry filter. The difference is slightly increasing with an increase of airflow rate and reaches a maximum for the airflow rate of 400 l/min. The difference in results for negative and positive inclinations at the same angle does not exceed 3%, however, the difference grows with an increase of angle.

4.3. Efficiency of filtration

Due to a very high stability of particle generation by the nebulizer and high accuracy of the Aerodynamic Particle Sizer, the reproducibility of the results was excellent and the discrepancy between two similar runs never exceeded 1%.

The average size distribution of particles produced by the nebulizer for 15 experimental runs is shown in Fig. 6. The majority of particles have diameters within the range from 0.56 to 1 μm. However, measurable numbers of bigger particles (diameter up to 1.24 μm) are also generated by the device.

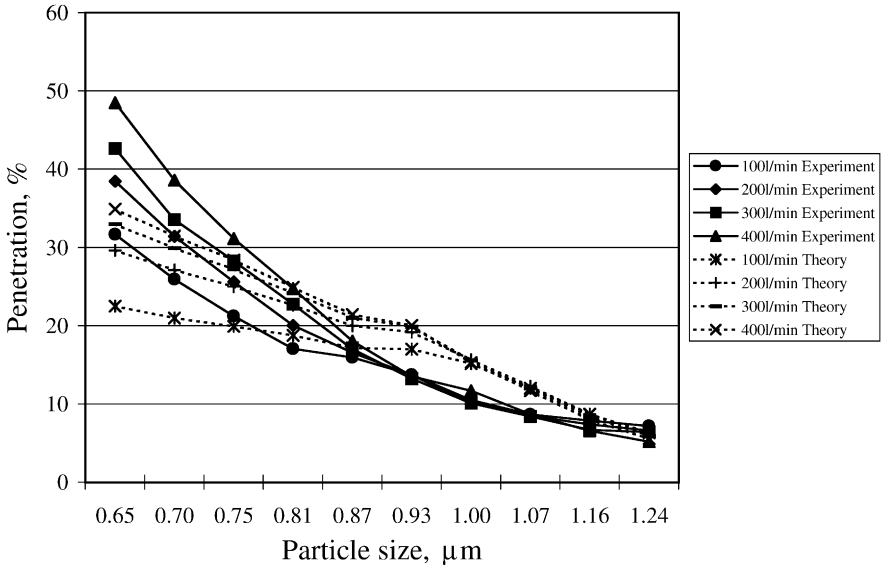

Fig. 7. Theoretical and experimental penetrations of dry filter as a function of aerosol particle size.

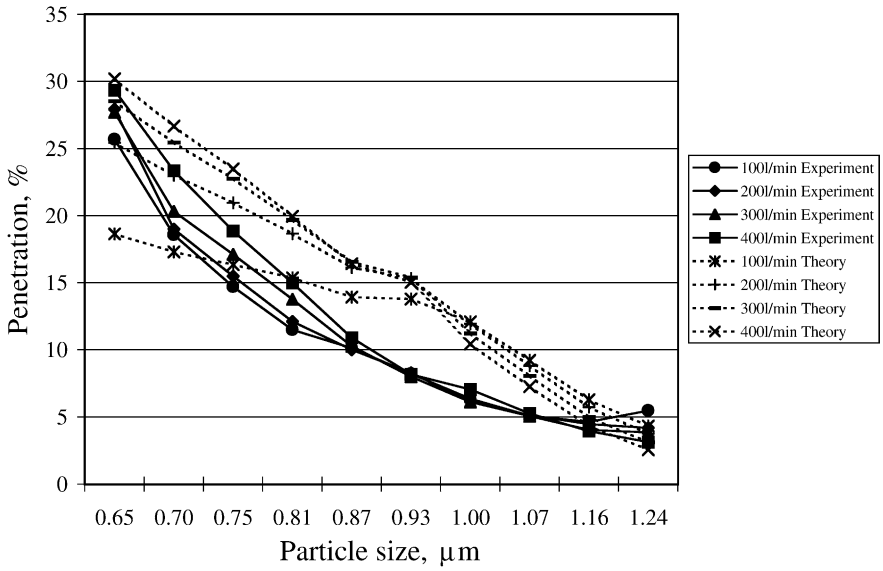

Fig. 8. Theoretical and experimental penetrations of wet vertical filter, as a function of aerosol particle size.

To obtain reliable data, the efficiency of filtration was also measured after stabilisation, after initiating a new flow regime. Measurements were made of the numbers of particles upstream and downstream of the filter, and the penetration estimated using Eq. (4). Note that this calculation uses "before" and "after" information, and is independent of any fluctuations in the output from the nebulizer. The theoretical equivalent packing densities were calculated using the established procedure of Agranovski and Braddock [4] and the theoretical penetration calculated using Eq. (4). The results of the theoretical calculations and the experimental measurements of the penetration of particles through the filtering system are presented in Figs. 7–12, for $G_L = 0.08$ kg/h.

Fig. 7 shows the penetration results for dry filtration. The experimental results were taken just after starting the process and when the filter was still dry. Obviously, for dry filtration θ does not make any difference, so the results were taken for the vertical arrangement only. The largest penetration was measured for the smallest particles for all air flow rates. The penetration is decreasing with increase in particle size and reached a minimum for the biggest particles with a diameter of 1.24 μm. The experimental estimates of the penetration are larger than the theoretical estimates for all flow rates and for the smaller particle sizes. The situation is reversed for the larger, up to 1.16 μm, diameter particles where the theoretical penetration is larger than the

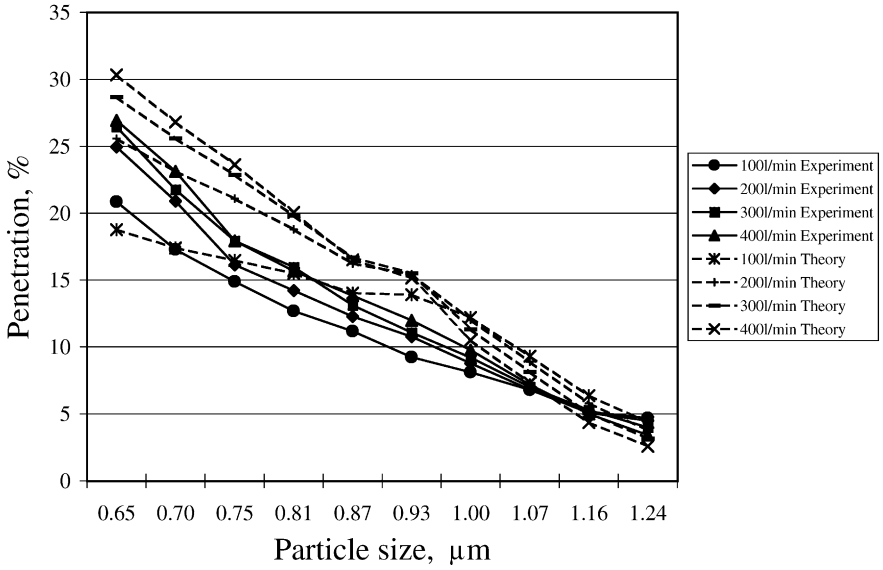

Fig. 9. Theoretical and experimental penetrations of wet filter as a function of aerosol particle size, for $\theta = 15^\circ$.

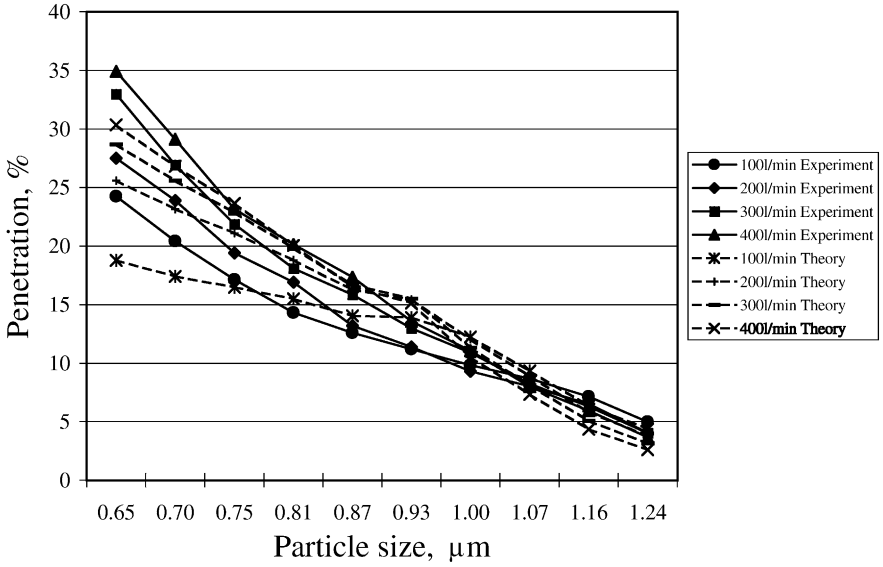

Fig. 10. Theoretical and experimental penetrations of wet filter as a function of aerosol particle size, for $\theta = -15^\circ$.

experimental values. However, theoretical and experimental values are very similar for the largest diameter of 1.24 μm.

Fig. 8 shows the percentage of penetration of particles through the vertically arranged wet filter. The results show a major decrease of penetration compared to the dry filtration process. The highest penetration is also occurring for the smallest particles for all air flow rates. However it is almost 50% lower than for the case of dry filtration. The three lower flow rates show that the theory underestimates the penetration for the smaller particle sizes. With increase in particle size, the theory overestimates the penetration for all flow rates. Again, the results of theory and experiment converge for the largest diameter of 1.24 μm.

The performance characteristics for four arrangements of the filter, i.e. $\theta = +15$, -15, $+30$ and -30° are presented in Figs. 9–12. As discussed before, the theoretical model does not distinguish between $\pm$ values of θ, and hence the theoretical curves on Figs. 9 and 10 ($\theta = \pm 15^\circ$) are the same. The theoretical values on Figs. 11 and 12 ($\theta = \pm 30^\circ$) are also the same. Generally, the penetration is larger for negative θ values than for corresponding positive ones; as is easily seen by comparing Figs. 9 and 10 for $\theta = \pm 15^\circ$ and Figs. 11 and 12 for $\theta = \pm 30^\circ$. The largest difference in values of experimental penetration for positive and negative inclinations were obtained for small diameter particles, but the differences become small for the larger particles, regardless of penetration.

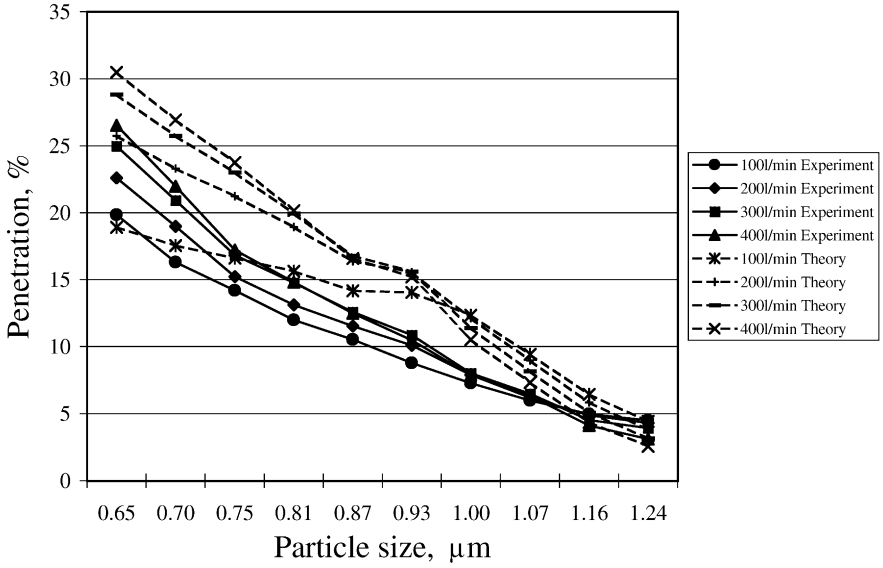

Fig. 11. Theoretical and experimental penetrations of wet filter as a function of aerosol particle size, for $\theta = 30^\circ$.

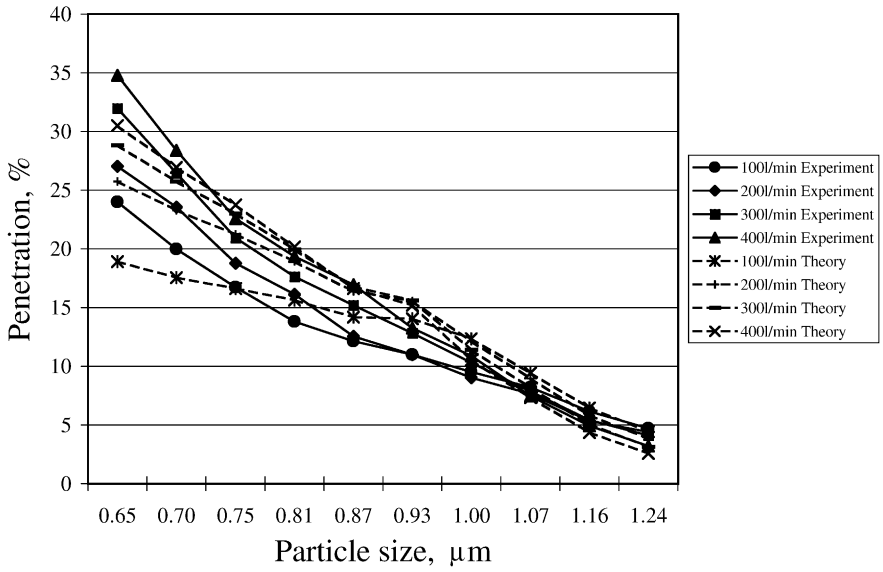

Fig. 12. Theoretical and experimental penetrations of wet filter as a function of aerosol particle size, for $\theta = -30^\circ$.

The experimentally measured penetrations also decrease by 2–6% from $\theta = 0$ to $+30^\circ$. For the negative inclinations, the experimental penetration results show fewer trends, with some increasing and some decreasing. For negative values of θ, the theoretical values of the penetration generally follow each other. For positive values of θ, the theoretical values of the penetration are generally larger than the observed values.

5. Discussion

Filtration of liquid particles on wettable fibrous filters is associated with the presence of liquid films covering each of the fibres. Tilting of the filter box can enhance the thickness and position of the film. Even for a relatively low irrigation rate of 0.08 kg/h, theoretically, the equivalent diameter of the fibre can be increased almost two times by inclining the filter by 85°. It corresponds to an increase in the packing density by a factor of 4. However, due to significant increase of the pressure drop across the filter, this inclination is not practical and was not covered by the experimental program. The theoretical equations were fully verified by the experiments for up to 30° inclinations in both positive and negative directions.

The theoretical and experimental results for the resistance of the filter are in excellent agreement. The development of the film is usually quick, of the order of 10 min (see Fig. 4), and the steady-state operation is relatively stable. Obviously, the resistance of the device for wet filtration is higher than for the dry one. For the vertical orientation, the theoretical pressure drop is slightly larger than the experimental pressure drop. The situation is reversed for the angled filter. These differences may arise from the assumptions about the structure of the filter not being fully valid. Tilting the filter may also enhance coalescence of films between fibres, thus increasing liquid hold up and increasing the resistance.

The penetration results show good agreement between the theoretical and experimental figures, for $\theta \leq 0$. For $\theta > 0$, the measured penetrations are lower, particularly for the smaller particles. The differences are small for larger particles. These differences may be due to accumulation of liquid in the filter, due to two factors. The first is that the bottom part of the filter is not freely located in, for example, a receiver but is fixed in the flange which introduces some problems for free drainage of liquid from the bottom of the filter.

The second and more important issue is that the model does not distinguish between $\theta > 0$ and $\theta < 0$ arrangements of the filter. However, the nature of the flow of captured liquid inside the filter for these two cases is different. Liquid captured by the filter is drained under the action of the component of gravitational force acting along the filter surface. The other component of the gravitational force, acting 90° to the surface of the filter, is directed parallel to and in the direction of the air stream for the $\theta < 0$ orientation. For $\theta > 0$, the gravitational component opposes the direction of airflow. For $\theta < 0$, the normal to the filter gravitational component and the drag of the air stream on the liquid films are acting in the same direction, and serve to push liquid deeper into the filter and even through it. A thicker film is associated with enhanced drainage down the fibres and as a result, the average thickness of the film across the filter is decreased.

The opposite situation occurs for $\theta > 0$ when the normal component of gravitational force is opposed to the direction of airflow. In this case, the liquid tends to accumulate more at the front of the filter but is pushed across the filter by the drag created by the air stream. The combination of oppositely acting forces redistributes liquid inside the filter more

uniformly and as a result, the average thickness of the film is bigger comparing to $\theta < 0$.

The efficiency of the device for $\theta > 0$ is always higher compared to $\theta < 0$ but for the same size angle. It can be explained by the variation in the thickness of the film and variations of the effective packing density which are dependent on the orientation. The $\theta > 0$ arrangement minimises the possibility of destroying the thick film located on the filter fibres at the rear of the filter, and minimises the possible removal of droplets generated as the result of the destruction. For $\theta < 0$, there is an increased possibility of destruction of the film on the fibre because of the greater drag acting on the film when air moves through the relatively low porosity rear of the filter with elevated velocity. The efficiency of the device is also increasing with an increase of the size of the angle of inclination.

6. Conclusion

Filtration of sticky particles, particularly by dry filters, can generate rapid build up of deposits on the filter and present major problems with cleaning and maintenance of the equipment. Where the aerosol is viscous, it may not be able to spread over the surface of the fibres and may not create the liquid film needed for enhanced filtration. Sometimes the aerosol is so dilute in the carrier gas, that it, by itself, is not able to form the required films on the fibres. In such cases, sprays of other liquids such as water can be used to generate liquid films on the fibres, and thus enhance the filtration of heavy viscous or even solid particles. The film acts as the primary filtration zone, removing particles before they reach the filter's surface and also decreases the effect of bouncing of particles after collision with the filter. Agranovski and Whitcombe [10] have used this approach to control the emissions from galvanising plants. They recommend that for exhaust streams heavily polluted by sticky liquid or solid particle aerosols, a low porosity filter be used in conjunction with the highest possible irrigation rates. It will provide films of maximum thickness and drainage, and will minimise blockage.

The tilting of the filter to retain fluid on the front face of the filter is of particular importance for industries where valuable irrigating liquids have to be used for the filtration process. It is also important for sites which have some limitations on the fresh liquid consumption. The possibility of utilising a smaller amount of fresh liquid utilised by the process also decreases costs.

References

[1] C.N. Davies, Air Filtration, Academic Press, London, New York, 1973.
[2] R.C. Brown, Air Filtration: An Integrated Approach to the Theory and Applications of Fibrous Filters, Pergamon Press, Oxford, 1993.
[3] I.E. Agranovski, Filtration of ultra-small particles on fibrous filters, Ph.D. Thesis, Griffith University, Brisbane, Australia, 1995.
[4] I.E. Agranovski, R.D. Braddock, Filtration of mists on wettable fibrous filters, AIChE J. 4 (12) (1998) 2775.
[5] I.E. Agranovski, R.D. Braddock, Filtration of mists on nonwettable fibrous filters, AIChE J. 4 (12) (1998) 2784.
[6] A. Kirsch, I. Stechkina, The theory of aerosol filtration with fibrous filters, in: D.T. Shaw (Ed.), Fundamentals of Aerosol Science, Wiley, New York, 1978.
[7] K.W. Lee, B.Y.H. Liu, Theoretical study of aerosol filtration in fibrous filters, Aerosol Sci. Tech. 1 (1982) 147–161.
[8] E. Schweers, F. Löffler, Realistic modeling of the behaviour of fibrous filters through consideration of filter structure, Powder Tech. 80 (1994) 191.
[9] W.C. Hinds, Aerosol Technology. Wiley, New York, 1999.
[10] I.E. Agranovski, J.M. Whitcombe, Utilisation of wet fibrous media for filtration of sticky aerosol particles, J. Aerosol Sci. 31 (2000) 204.